Vibrational Spectroscopy 55 (2011) 107–114

Contents lists available at ScienceDirect

Vibrational Spectroscopy

journal homepage: www.elsevier.com/locate/vibspec

Infrared spectra of β-hydroquinone–xenon crystal. H/D isotope and temperature effects

M. Ilczyszyn[a,*], M. Selent[a,b], M.M. Ilczyszyn[a], J. Baran[c]

[a] Faculty of Chemistry, Wrocław University, 50-383 Wrocław, Joliot Curie 14, Poland
[b] Department of Physical Sciences, University of Oulu, 90014 Oulu, Finland
[c] Institute of Low Temperature and Structure Research of Polish Academy of Science, 50-950 Wrocław, ul. Okólna 2, Poland

ARTICLE INFO

Article history:
Received 25 June 2010
Received in revised form
14 September 2010
Accepted 16 September 2010
Available online 20 October 2010

Keywords:
Hydroquinone
Xenon
Clathrate
Hydrogen bond
Isotope effect
Infrared spectra

ABSTRACT

Preliminary infrared studies of the host–guest interactions in the β-hydroquinone–Xe clathrate are reported. The infrared spectra of the normal and deuterated compounds are analysed at various temperatures. Normal vibrations of the host H-bonds are found to be very sensitive on the interactions with the Xe guest atoms. The temperature induced escape of the Xe from the normal and deuterated crystals appears at different temperatures and is responsible for different changes of the γOH and γOD deformation mode frequencies, respectively. In both cases the β-hydroquinone crystals with empty cages are formed in the first step and then they are transformed into their α-modifications.

1. Introduction

Three crystalline modifications of hydroquinone (HQ) are known: α-, β- and γ-HQ. The main differences between them can be related to their H-bond networks [1–4]. In the β modification, almost spherical cavities are formed between successive hexagonal rings of coupled H-bonds: $[\cdots O–H\cdots O–]_6$. Some atoms or small molecules, such as Ar, Kr, Xe, CO_2, H_2, N_2, O_2, HCl, H_2S, HCO_2H, CH_3OH, etc. can be trapped in these cavities [4]. In the α-HQ crystal two structural motifs, tied together by weak H-bonds, can be distinguished: (i) cages formed between hexagonal rings of H-bonds—of the same type as cages in the β-HQ; (ii) a double helix of chains of the HQ molecules around the screw axes [2]. In the monoclinic γ modification, the HQ molecules are only linked by H-bonds into infinite helices around the screw axes [3]. Among these three HQ crystalline modifications, only the α-HQ crystal is stable at the room temperature; the β-HQ and γ-HQ crystals spontaneously change into the α-HQ modification. Particularly, the β-HQ form is stabilized by the host–guest interactions and it converts to the α-HQ one after the guest release.

Among these three HQ crystalline modifications, the β-HQ one currently attracts special attention for its ability to form inclusion compounds, which illustrate the inclusion phenomena as very important in biochemistry, biology, agricultural, and pharmaceutical areas [5]. Particularly, the β-HQ–Xe clathrate appears to be appropriate model for the study of the interactions between the Xe atom and H-bond systems. It seems to be very important because the Xe gas is known as excellent anaesthetic material [6].

Many investigations of the IR spectra of the β-HQ clathrates with encaged guest molecules (O_2, HCN, CO_2, H_2S, etc.) as well as detailed analysis and interpretation of intramolecular vibrations and external modes of the guest molecules have been available so far in the literature [7–15]. Studies concerning internal vibrations of the β-HQ crystal filled up by the Xe atoms (β-HQ–Xe) have not been reported. Only three papers on the vibrational spectra of the β-HQ–Xe crystal in the region of lattice vibrations have been available to date [11,13,15].

In this contribution we would like to check utility of the IR spectroscopy (in the middle range) to studies of the β-HQ (host)–Xe (guest) interactions. The basic assumption of our treatment is as follows: every enclosed Xe atom is rigidly fixed at an equilibrium site within the cage and it affects vibrations of the host. Our attention is focused on the H-bond vibrations as well as on selected HQ internal vibrations. In order to achieve our aim the following actions were undertaken and described below:

(i) In the first section, the IR spectra of both β-HQ–Xe and β-DQ–Xe crystals (i.e. with natural isotopic content and

* Corresponding author. Tel.: +48 71 3757332; fax: +48 71 3282348.
E-mail addresses: mi@wchuwr.chem.uni.wroc.pl, mi@wchuwr.pl (M. Ilczyszyn).

0924-2031/$ – see front matter © 2010 Elsevier B.V. All rights reserved.
doi:10.1016/j.vibspec.2010.09.005

deuterated one, respectively) at the room temperature are analysed. It is preceded by our theoretical investigation of the geometry and vibrational frequencies of isolated HQ and DQ molecules. These calculations indicate possible couplings between internal vibrations of hydroquinone and support our assignments based on the data available in the literature [12,13,16,17]. Generally, our infrared spectrum of the β-HQ–Xe crystal is close to the β-HQ spectrum recently reported by Kubinyi et al. [13]. However, they differ in some points.

(ii) In the next section the temperature influence on the infrared spectra of the β-HQ–Xe and β-DQ–Xe crystals is considered. These studies were performed in the wide temperature range: from 11 to 448 K (melting). In this section, the influence of the Xe escape on the infrared spectra of both β-HQ–Xe and β-DQ–Xe crystals is also discussed.

(iii) Summary is given in the last section.

2. Experimental and computational details

Two β-HQ–Xe samples were prepared by sublimation of commercially available α-HQ crystal in the xenon atmosphere at the pressure of 20 atm. Their deuterated analogues (β-DQ–Xe) were prepared by sublimation of the α-DQ crystal in the xenon atmosphere at the same pressure. α-DQ was obtained by three-fold crystallization of commercially available α-HQ from D_2O. In the α-DQ and β-DQ–Xe crystals only protons of the hydroxyl groups are substituted by deuterons and ca. 85% degree of this enrichment was estimated by the IR method. One pair of our samples, β-HQ–Xe and β-DQ–Xe, were used for the measurements below the room temperature, the second one for the higher temperature experiments.

As follows from the high temperature IR spectra, only the β-HQ–Xe sample was not contaminated with α-HQ. All the remaining samples contained small amounts of the α crystalline modification.

The infrared spectra of both β-HQ–Xe and β-DQ–Xe samples at different temperature were measured by means of a Bruker IFS-88 FT-IR and Bruker IFS-66 FT-IR spectrometers operating with 2 cm^{-1} resolution. The powder samples were prepared as Nujol mulls on KBr windows or KBr pallet. The low temperature spectra from 11 to 300 K were recorded using a closed helium cryostat (ARS Displex Model CS202-X1.AL closed cycle cryostat) to which a temperature controller of Scientific Instruments (Model SI-9700-1) was joined; (ii) the high temperature infrared spectra from 298 to 448 K were measured by means of the Specac high temperature cell. The temperature dependent IR spectra were recorded in the following way:

(i) *The low temperature spectra.* The first spectrum was recorded at 11 K, then the sample was heated step-by-step, up to the room temperature. The maximum temperature variation in one step was 20 K and the waiting time for the temperature stabilization was 20 min.

(ii) *The high temperature spectra.* The spectra in this region were measured from the room temperature up to 448 K, using analogous step-by-step procedure.

The room temperature FT-Raman powder spectra of both β-HQ–Xe and β-DQ–Xe samples were measured using a Nicolet IFS-860 instrument with a Raman attachment and a Nd:YAG laser pumped by a diode laser (λ = 1064 nm, power ca. 300 mW). The spectral resolution was 2 cm^{-1}.

Thermal analysis of the β-HQ–Xe and β-DQ–Xe crystals under nitrogen atmosphere was performed from ca. 300 K to ca. 675 K using thermogravimetric–differential thermal analyzer (Setaram SETSYS 16/18 instrument). The heating rate at 2 °C/min was used.

Our B3LYP/6-311++G (2d, 2p) calculations for isolated HQ and DQ molecules were performed with the Gaussian 03 package of computer codes [18]. The harmonic vibrational frequencies were calculated following the structure optimizations together with the infrared intensities and Raman scattering activities.

3. Results and discussion

3.1. Crystal structure

The β-HQ–Xe clathrate crystallizes in the $R\bar{3}$ space group of trigonal system, $Z = 3$ [4]. The HQ molecules are linked together by intermediate/weak O–H···O bonds of R(O···O) = 2.705 Å length. The main structural motif is nearly spherical cavity built out of six interlocking C_6H_4 moieties and two hexagonal rings of coupled H-bonds, $[\cdots O–H\cdots O–]_6$, placed on the other side of it. In considered crystal the Xe atoms are trapped as the guests. These cavities fit tight, i.e. each H-bonded hexagonal ring simultaneously belongs to two cages, thus forming the columns running parallel to the crystal *c* axis. In deuterated crystal, β-DQ–Xe, only protons of the hydroxyl groups are replaced by deuterons and similar crystal structure with $[\cdots O–D\cdots O–]_6$ hexagonal rings is expected here.

3.2. Infrared spectra

3.2.1. Room temperature IR spectra of β-HQ–Xe and β-DQ–Xe crystals

The wavenumbers of the bands observed in the infrared and Raman spectra of the β-HQ–Xe, β-DQ–Xe, α-HQ and α-DQ polycrystalline samples are given in Table 1. The theoretical band positions, infrared intensities (I_{IR}) and Raman scattering activities (S_R) of isolated HQ and DQ molecules (only protons in the hydroxyl groups are substituted by deuterons) are also listed there. The band assignment given in the last column is based on the vibrational data obtained for: (i) the β- and α-HQ crystalline modifications [12,13]; (ii) selected derivatives of benzene [16,17]; (iii) isolated HQ and DQ molecules (our theoretical calculations). The experimental FT-IR and Raman powder spectra of the β-HQ–Xe and β-DQ–Xe samples recorded at the room temperature are shown in Fig. 1. Spectroscopic data for the β-HQ–Xe crystal reported below are, in many regions, similar to those obtained by Kubinyi et al. [12,13] for the β-HQ modification. In some cases, significant differences are noted.

3.2.1.1. Hydrogen bond vibrations. The νOH stretching vibration of the β-HQ–Xe crystal gives rise to the broad and intense infrared band at 3160 cm^{-1}. Similar IR absorption was observed by Kubinyi et al. [12,13]. for the β-HQ crystal. For the β-DQ–Xe crystal, corresponding intense band, νOD, is observed at 2372 cm^{-1}. The isotopic frequency ratio νOH/νOD is equal to 1.33 and indicates medium OHO H-bonding [19].

The δOH in-plane deformation mode of the OHO H-bond, as follows from our theoretical calculations, is strongly coupled to the aromatic ring vibrations, namely to the νCC and δCH modes, and gives significant contribution to three infrared absorptions apparent in the following regions: 1552–1413, 1395–1287 and 1268–1130 cm^{-1}. The pattern of the IR absorption in above regions is significantly influenced by deuteration; its intensity is reduced and the maxima of the bands are noticeably shifted to the lower or higher wavenumbers (Fig. 1, Table 1). Simultaneously, in the infrared spectrum of the β-DQ–Xe crystal a new intensive absorption in the 1052–858 cm^{-1} region with two maxima at 988 and 975 cm^{-1} appears. It has been assigned to the δOD mode. This vibration, similarly to the δOH one, is coupled to the aromatic ring vibrations. Presented suggestions are confirmed by our calculations for isolated HQ and DQ molecules. Determination of the δOH/δOD

Table 1
Comparison of the experimental wavenumbers (cm^{-1}) of the infrared and Raman bands of crystalline β-HQ–Xe clathrates and its deuterated analogue (β-DQ–Xe) and theoretical harmonic wavenumbers (ν, cm^{-1}), intensities (I_{IR}, km/mol), Raman scattering activities (S_R, $Å^4$/amu) and Raman intensities (I_R) calculated for HQ and DQ molecules at B3LYP/6-311++G(2d,2p).

β-HQ–Xe crystal		Isolated HQ molecule				β-DQ–Xe crystal		Isolated DQ molecule		α-HQ crystal	α-DQ crystal	Bands assignment[b]
Experimental		Calculated				Experimental		Calculated		Experimental		
Infrared	Raman[a]	ν	I_{IR}	S_R	I_R	Infrared	Raman[a]	ν	I_{IR}	Infrared	Infrared	
		3845	0	205	51					3257 vs b	3235 w b	νOH
3160 s b		3844	126	0	0	3190 m b				3162 vs b	3182 w b	νOH
	3063 (29)	3202	0	244	112		3062 (65)	3202	0			$\nu_2(\nu CH)$
3064 s sh		3200	7	0	0	3064 m		3200	7			$\nu_{20}(\nu CH)$
	3047 (9)	3162	0	180	86	3039 m	3042 (24)	3162	0			$\nu_7(\nu CH)$
3030 s		3160	28	0	0	3027 m		3160	30	3028 vs		$\nu_{20}(\nu CH)$
	3018 (4)					3022 m						
						3007 m	2997 (5)					
2720 m						2725 w				2723 m		
2698 m						2698 vw				2690 m		
2595 w										2607 m		2xδOH
						2588 vw	2576 (3)					
2565 sh w												2xδOH
						2536 vw						νOD?
2460 w										2460 w	2462 m sh	νOD
						2448 m sh						νOD?
						2405 s sh	2412 (7)	2799	0		2426s	νOD
						2372 vs	2350 (6)	2798	81		2394 s	νOD
						2288 m sh					2350 m sh	νOD?
						2071 w						νOD?
2011 vw										2016 vw		
						1993 w						2xδOD
						1953 w						2xδOD
1870 vw						1870 w				1870 vw		
1855 vw										1855 vw		
						1753 vw						
1648 vw	1619 (12)	1664	0	12	26	1646 vw	1625 (3)	1660	0	1626 vw		$\nu_8(\nu CC)$
1609 vw	1596 (17)	1644	0	9	1		1609 (13)	1634	0	1609 vw		$\nu_8(\nu CC)$
							1592 (15)					
						1540 vw						
1517 s		1551	167	0	0	1510 vs		1545	246	1516 vs	1507 vs	$\nu_{19}(\nu CC)$
						1501 vs						$(\nu_{19})(\nu CC)$
1450 sh		1490	99	0	0	1428 s		1465	13			$\nu_{14}(\nu CC) + \delta OH/\delta OD$
1363 m	1363 (2)	1371	0	2	5	1296 vw	1304 (7)	1340	0	1366 vs		$\nu_3(\delta CH) + \delta OH/\delta OD$
										1354 vs		$\nu_3(\delta CH) + \delta OH/\delta OD$
1345 m sh		1355	41	0	0	1287 w		1324	12		1286 m	$\delta OH/\delta OD + \nu_{18}(\delta CH)$
1331 w sh										1334 s sh		$\delta OH + \nu_{18}(\delta CH)$
										1316 m sh		
											1310 w	
	1256 (24)	1280	0	28	94		1255 (22)	1271	0	1259 s	1260 s	$\nu CO + \nu_{14}(\nu CC)$
1245 s		1262	196	0	0	1242 vs	1241 (4)	1258	265	1243 vs	1238 s sh	$\nu_{12}(\delta CCC) + \nu CO$
											1232 vs	
										1220 vs		$\delta OH + \nu_3(\delta CH)$
1210 s	1221 (2)	1199	0	12	46	1225 vs				1209 vs	1210 vs	$\delta OH + \nu_3(\delta CH)$
	1159 (23)	1185	0	5	19		1160 (20)	1185	0			$\nu_9(\delta CH)$
1194 vs		1181	269	0	0	1208 s				1191 vs		$\delta OH + \nu_{18}(\delta CH)$
										1164 s		$\delta OH + \nu_{18}(\delta CH)$
1121 w										1118 m		
						1106 m					1106 m	$\nu_{18}(\delta CH)$
1095 s		1117	40	0	0	1099 m		1127	21	1096 s	1100 m	$\nu_{18}(\delta CH) + \delta OH/\delta OD$
											1030 m	
1009 w		1027	0	0		1009 m		1027	0	1009 w	1009 m	$\nu_{18}(\delta CH)$ (?)
						988 s		946	0		991 s	$\delta OD + \nu_3(\delta CH)$
										970 vw		
947 vw		939	1	0	0	948 m sh		938	1			$\nu_{17}(\gamma CH)$
942 vw						943 m sh				940 vw	939 m	$\nu_{17}(\gamma CH)$
						975 m		923	174		968 s	$\delta OD + \nu_{18}(\delta CH)$
919 vw		911	0	0	0			911	0	920 vw	918 w	$\nu_{10}(\gamma CH)$
898 vw	852 (48)	863	0	46	283		849 (21)	857	0			$\nu_1(\nu CC) + \nu CO$
										890 vw		
833 s	832 (36)	828	66	0		832 vs	829 (40)	828	69	829 s	829 s	$\nu_{11}(\gamma CH)$
										826 s	823 vs	$\nu_{11}(\gamma CH)$
	811 (6)	797	0	1	4		811 (6)	796	0			$\nu_{10}(\gamma CH)$
										765 vs sh		
760 s		763	64	0	0	747 vs		752	38	758 vs	748 vs	$\nu CO + \nu_{12}(\delta CCC)$
740 m sh										737 s		
						701 vw	704 (3)			701 m		$\nu_4(\gamma CCC)$
	697 (2)	695	0	2	12			694	0	691 m sh		$\nu_4(\gamma CCC)$
	645 (16)	660	0	6	49		642 (13)	657	0			$\nu_6(\delta CCC)$
											553 w	

Table 1 (*Continued*)

β-HQ–Xe crystal		Isolated HQ molecule				β-DQ–Xe crystal		Isolated DQ molecule		α-HQ crystal	α-DQ crystal	Bands assignment[b]
Experimental		Calculated				Experimental		Calculated		Experimental		
Infrared	Raman[a]	ν	I_{IR}	S_R	I_R	Infrared	Raman[a]	ν	I_{IR}	Infrared	Infrared	
526 m		514	25	0	0	517 w		514	20	525 m		$\nu_{17}(\gamma CH)$
										517 m	515 m	$\nu_{17}(\gamma CH)$
										487 vw		
										476 vw		
	484 (6)	473	0	8	112		466 (8)	466	0	465 vw		$\nu_6(\delta CCC)$
										460 vw		
	475(9)	449	0	1	4		459sh	426	0			$\nu_{15}(\delta CH)+\delta CO$
											445 m	
430 vw	457 (8)	427	5	0	0		445 (4)	425	1			$\nu_{16}(\gamma CCC)$
										410 vw		
	375 (17)	361	0	2	38		374 (16)	360	0			$\nu_5\ (\gamma CH)+\gamma CO$
	380 (11) sh	341	17	0	0			321	17			$\nu_{9b}(\delta CH)+\delta CO$
685 w b		276	197	0.1	1							τOH/γOH
		276	2	3	59					613 w b		τOH/γOH
						550 w		207	104			τOD/γOD
						494 w		203	0			τOD/γOD
											471 w	τOD/γOD
	210 (10)	153	1	0			205 (9)	146	5			$\gamma CO_H/\gamma CO_D$
	99 (100)						101 (100)					Lattice mode

Abbreviations: ν, stretching; δ, bending in plane; γ, bending out of plane; τ, torsion; vs, very strong; s, strong; m, medium; w, weak; vw, very weak; sh, shoulder; and b, broad.

[a] Relative Raman band intensities are given in parentheses. The intensity of the most intense band in the spectrum was assumed as 100.

[b] The bands derived from the aromatic ring vibrations are denoted according to Refs. [16,17]. In parentheses, the vibration which gives the main contribution to the corresponding normal vibration of the aromatic ring, is given. The notation δOH/δOD means that δOH or δOD contribute into given vibration for the non-deuterated or deuterated sample, respectively.

isotopic frequency ratio from our experimental spectra was impossible due to the couplings of the δOH and δOD vibrations with other modes.

The out-of-plane γOH, contrary to the δOH one, is not coupled to other skeletal modes and appears in the IR spectrum as a weak and broad band at 685 cm^{-1}. On deuteration it shifts to 550 cm^{-1}. The γOH/γOD isotopic frequency ratio is equal to 1.26.

3.2.1.2. Aromatic ring vibrations. As follows from Kubinyi et al. [12,13] and from our calculations, the majority of the aromatic ring vibrations are complex and coupled with the H-bond and hydroxyl vibrations. These couplings result in changing of the band positions when the hydroxyl groups are deuterated. This feature is predicted by our calculations and confirmed by our experimental data. Thus, the vibrations with significant contribution of the hydroxyl groups are very sensitive to the isotopic substitution. Distinctly, the bands derived from the aromatic ring vibrations, in which the C–O group participates, exhibit small variations in frequency. There are also some bands which keep the same position in the infrared spectra of both deuterated and non-deuterated species. They are not coupled to the O–H, O–D and/or C–O modes. The detailed assignment of the aromatic ring vibrations is presented in Table 1.

3.2.2. Comparison of IR spectra of β-HQ–Xe and α-HQ crystals at room temperature

In this contribution our attention is mainly focused on the β-HQ–Xe and β-DQ–Xe clathrates and on the host–guest interactions. But one should note that our samples (with one exception) were slightly contaminated with the α-HQ or α-DQ, respectively. Additionally, we observe the β → α transformation of the crystals at the highest temperatures used here. Thus, the key problem in this study is a discrimination between the bands arising from the α and β modifications. Assignments presented below are based on comparison of the IR spectra of the α-HQ, α-DQ, β-HQ–Xe and β-DQ–Xe samples (Table 1).

As follows from the vibrational data reported by Kubinyi et al. [13], the infrared spectrum of the α-HQ crystal is more complex than the spectrum of the β-HQ modification due to three non-equivalent HQ molecules in the asymmetric unit cell of the α form [2]. This expectation is confirmed by our spectra (Figs. 2 and 3). In spite of this, only a few spectral regions might be used for monitoring of the α-HQ content in the samples studied here. Besides the bands due to the H-bond vibrations (νOH and γOH), the absorption apparent in the region 1300–1150 cm^{-1} and bands at ca. 520 cm^{-1} seem to be handy for differentiation between the α- and β-HQ modifications.

Thus the β-HQ–Xe crystal can be identified by three groups of the bands: (i) the H-bond ones at 3160 (νOH) and 685 (γOH) cm^{-1}; (ii) three strong bands at 1245, 1210 and 1194 cm^{-1}; (iii) one band at 526 cm^{-1}. The corresponding bands for the α-HQ form are observed at: (i) 3162, 3257 (νOH) and 613 (γOH) cm^{-1} (weaker H-bonds are apparent in the α-HQ modification [2,19]); (ii) 1259, 1243, 1220, 1209, 1191 and 1164 cm^{-1} (six strong bands); (iii) 525 and 517 cm^{-1} (the latter band exhibits higher intensity than the former one).

Smaller differences are observed between the IR spectra of the α-DQ and β-DQ–Xe crystals (Fig. 3). Most bands exhibit almost the same positions and similar shape. Some differences concern the D-bond vibrations (νOD in the 2500–2000 cm^{-1}, δOD in the 1000–900 cm^{-1} and γOD in the 600–450 cm^{-1} regions) and the aromatic ring vibrations in the 1250–1190 cm^{-1} (ν_{12}, ν_3, ν_{18}) and 950–900 cm^{-1} (ν_{17}) regions. The most characteristic difference between the α-DQ and the β-DQ–Xe spectra refers to two bands

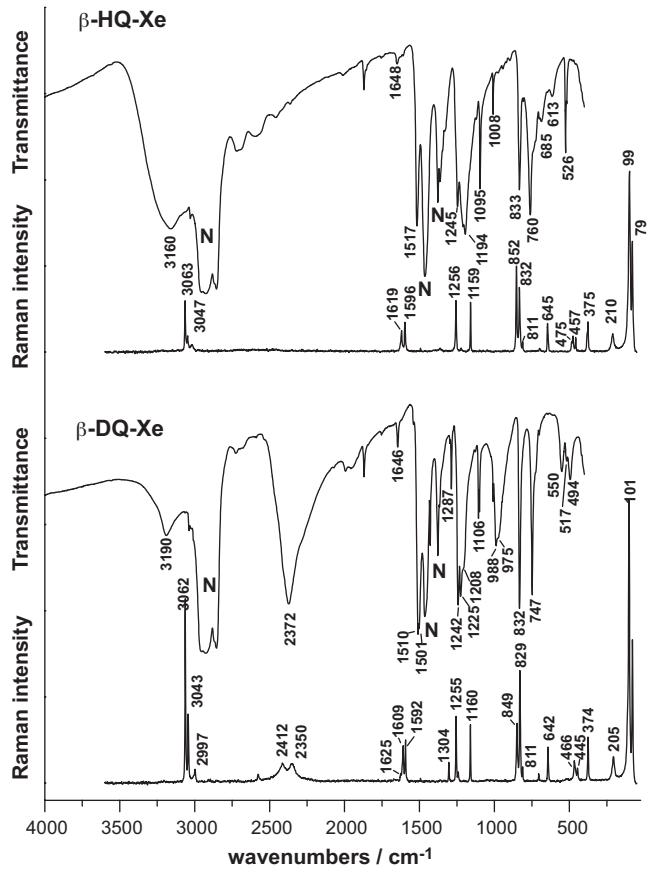

Fig. 1. The infrared and Raman spectra of the β-HQ–Xe (upper) and β-DQ–Xe (lower) polycrystalline samples measured as Nujol mulls (N—Nujol absorption) at the room temperature.

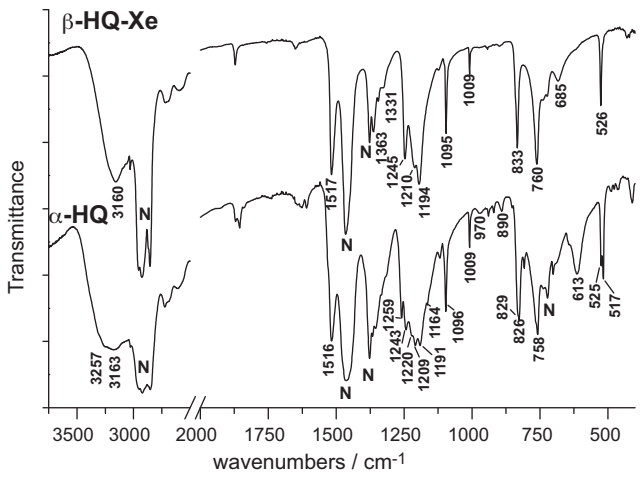

Fig. 2. Selected regions of the infrared spectra of the β-HQ–Xe (upper) and α-HQ (lower) polycrystalline samples measured as Nujol mulls (N—Nujol absorption) at the room temperature.

at 1310 and 1030 cm^{-1}, which are only present in the spectrum of the α-DQ crystal. Their origin is unclear.

3.2.3. Temperature dependent IR spectra of β-HQ–Xe and β-DQ–Xe crystals

3.2.3.1. Low temperature IR spectra. Selected infrared spectra of the β-HQ–Xe and β-DQ–Xe samples recorded below the room temperature are shown in Figs. 4 and 5, respectively. The wavenumbers of the IR bands observed therein are listed in Tables S1a and S2a, respectively.

Significant changes in the spectra of the β-HQ–Xe clathrate were found in two regions of the H-bond vibrations (νOH: 3500–3000 cm^{-1}, and γOH: 700–500 cm^{-1}) and combination $\nu CO + \nu_{12}$ mode region (ca. 760 cm^{-1}) as the crystal was heated up from 11 K to the room temperature (Fig. 4, Table S1a). The maximum of the νOH band progressively shifts to the higher wavenumbers, from 3074 cm^{-1} at 11 K to 3160 cm^{-1} at 300 K, while the band due to the γOH mode shifts in the opposite direction, from 717 to 685 cm^{-1}. Simultaneously, three submaxima observed on the νOH absorption at 11 K (3274, 3211 and 3147 cm^{-1}) disappear during the heating up. Similar variations concern three components of the $\nu CO + \nu_{12}$ band at 795, 769 and 756 cm^{-1}. All these components shift to the lower wavenumbers when the temperature increases and the first one disappears at 210 K. The position of the remaining infrared bands arising from the internal vibrations of the aromatic ring and the hydroxyl groups are not changing on the heating up. Some of them became much broader and less intense.

Similar temperature variations, as described above, one can notice in the IR spectra of the β-DQ–Xe crystal (Fig. 5, Table S2a). Significant changes concern the absorption arising from the D-bond vibrations, namely the νOD band shifts from 2323 to 2365 cm^{-1}, the δOD from 1002 to 988 cm^{-1} and the γOD from 587 to 550 cm^{-1} when the sample is heated up from 11 to 300 K. But the bands originating from the aromatic ring internal vibrations show only small changes.

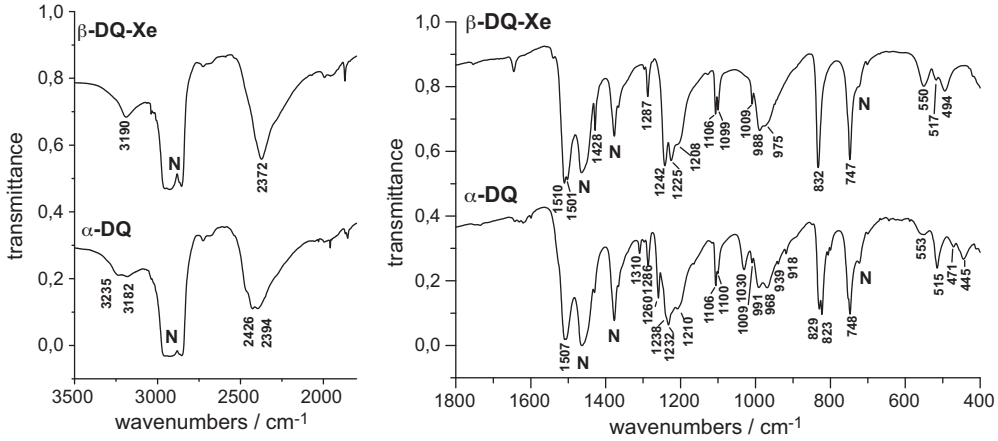

Fig. 3. The high and low frequency regions of the infrared spectra of the β-DQ–Xe (upper) and α-DQ (lower) polycrystalline samples measured as Nujol mulls (N—Nujol absorption) at room temperature.

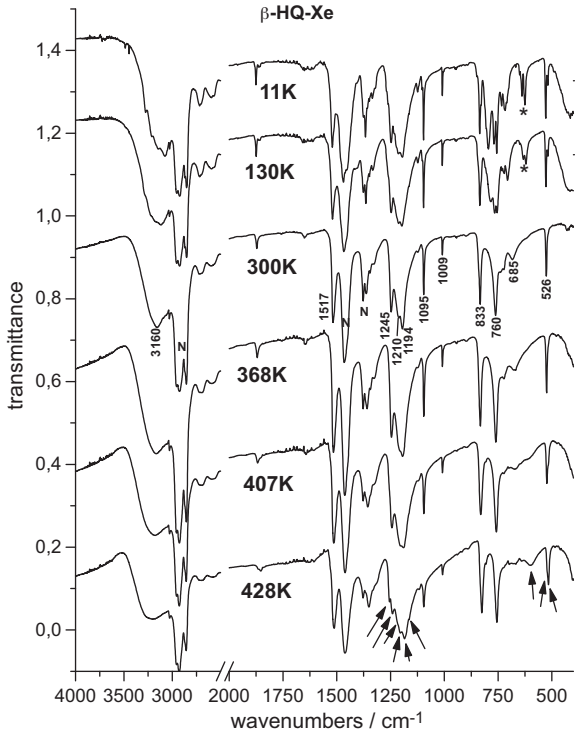

Fig. 4. The infrared spectra of two β-HQ–Xe polycrystalline samples measured as Nujol mulls (N—Nujol absorption) at different temperatures. Stars denote the bands arising from the α-HQ contamination, arrows denote α-HQ bands observed after the Xe escape.

3.2.3.2. Temperature induced Xe escape and $\beta \rightarrow \alpha$ transformation. We are interested in behavior of considered clathrates when the β-HQ–Xe and β-DQ–Xe crystals are heated up to the Xe escape temperature and next to their melting at ca. 447 K. We consider two possible scenarios to occur:

(i) The meta-stable β-HQ* and β-DQ* crystals with empty cavities are formed in the first step [20], which are next converted into the stable α-HQ and α-DQ modifications (respectively) in the second step;
(ii) The $\beta \rightarrow \alpha$ phase transition and the Xe escape appear to be one coupled process.

The infrared spectra of the β-HQ–Xe and β-DQ–Xe crystals at selected temperatures above 300 K are depicted in Figs. 4 and 5, respectively. Positions of all bands apparent in our spectra recorded above the room temperature are listed in Tables S1b and S2b.

Only slight changes in the IR absorption are found when the β-HQ–Xe sample is heated up from 298 to 398 K (Fig. 4, Table S1a). The broad absorption due to the νOH vibration shifts from 3160 cm^{-1} at 298 K to 3168 cm^{-1} at 398 K. The bands derived from coupled vibrations: $\nu_{12} + \nu$CO and δOH + ν_3 change their positions: from 1245 to 1244 cm^{-1} and from 1210 to 1206 cm^{-1}, respectively. The γOH band is observed at 685 cm^{-1} at 298 K and it shifts to 670 cm^{-1} at 398 K. As expected for β-HQ–Xe, only one band due to the ν_{17} mode at 526 cm^{-1} is apparent.

In the 407–413 K temperature range a new broad band at ca. 610 cm^{-1} appears, instead of the γOH band at 670 cm^{-1} observed at 398 K, while the remaining infrared bands show the same shapes and almost the same positions as in the spectra measured below 407 K. This new band is assigned by us to the γOH vibration of empty β-HQ* crystal (deprived of the Xe guests). Thus, the jumping of the γOH band from ca. 670 to 610 cm^{-1} at ca. 410 K is attributed

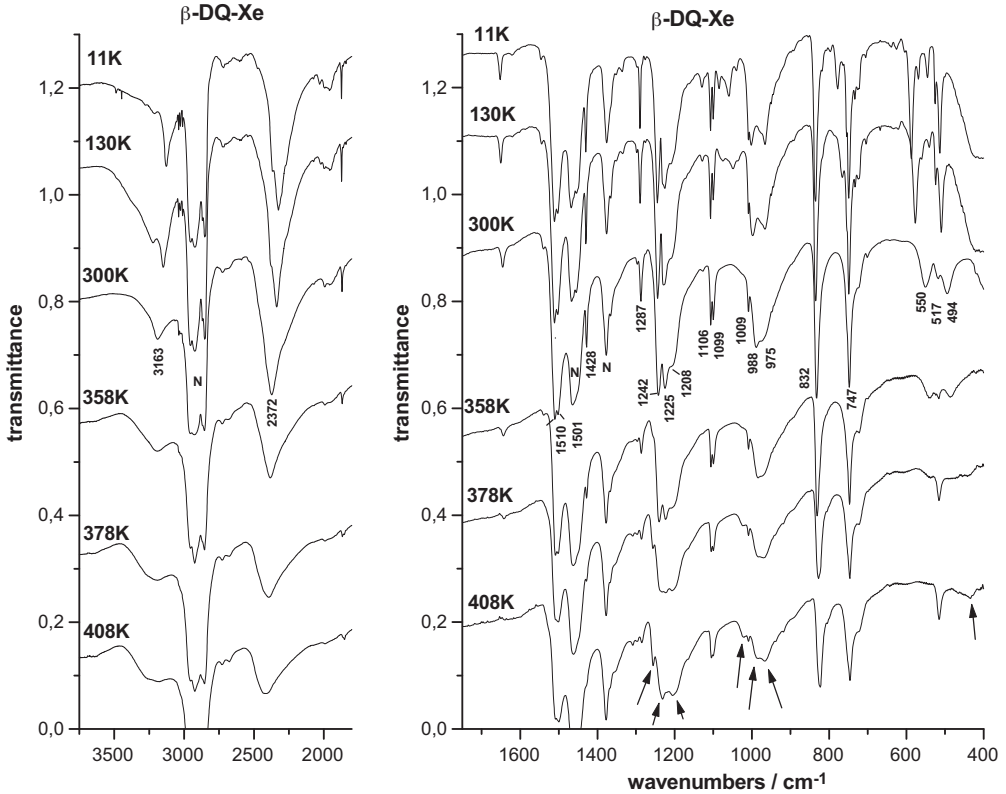

Fig. 5. The high and low frequency regions of the infrared spectra of the β-DQ–Xe polycrystalline sample measured as Nujol mulls (N—Nujol absorption) at different temperatures. Arrows denote α-HQ bands observed after the Xe escape.

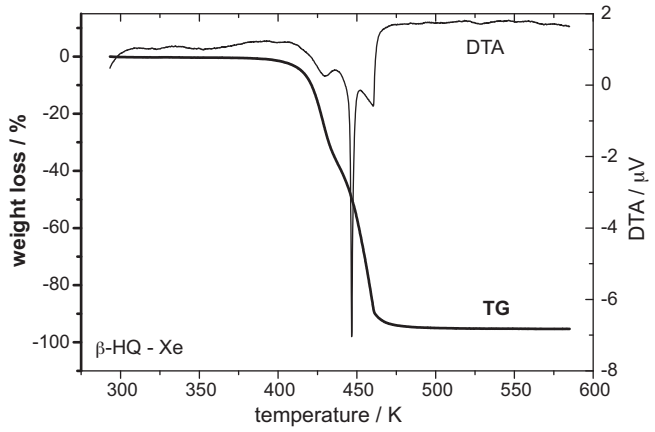

Fig. 6. The TG and DTA thermograms for the β-HQ–Xe crystal taken in the 300–600 K temperature range.

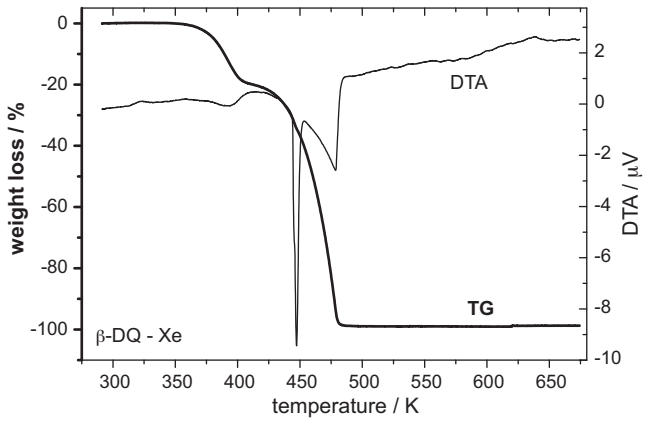

Fig. 7. The TG and DTA thermograms for the β-DQ–Xe crystal taken in the 300–675 K temperature range.

by us to the Xe escape from the β-HQ–Xe crystal and clearly shows on the host–guest interaction (its nature will be considered in our separate paper).

Our independent TG–DTA experiment confirms this interpretation. As follows from Fig. 6, the β-HQ–Xe crystal is stable up to ca. 400 K. The Xe escape around 429 K is detected by the broad, endothermal peak on the DTA curve and by the jump on the TG curve due to the sample weight loss. The sharp endothermal peak on the DTA curve at ca. 447 K and broader one at ca. 461 K indicate two additional processes: the crystal melting and its vaporization (the boiling point is expected at 560 K), respectively. Unfortunately, it is difficult to estimate the Xe atoms content in this clathrate due to the overlapping of two successive jumps on the TG curve: corresponding to the Xe escape and to the vaporization. Finally, one should note that this method reveals the beginning of the Xe escape at slightly higher temperature relative to the temperature based on our IR spectra—it can be explained by different sensitivity of both methods and different heating procedures in our TG–DTA and IR experiments (see Section 2).

Significant changes are observed in our IR spectra when the sample is heated up above 418 K (Fig. 4, Table S1b). Three new bands are observed in the 1300–1150 cm^{-1} region and this IR absorption is close to the absorption apparent in the α-HQ infrared spectrum. The band assigned to the γOH vibration of empty β-HQ* crystal (610 cm^{-1} at 407–413 K) shifts to 597 cm^{-1} at 438 K—the last position is characteristic for the γOH band in the α-HQ infrared spectrum. The band at 526 cm^{-1} transforms into the strong band at ca. 516 cm^{-1} with the shoulder at 523 cm^{-1} above 418 K. Such features are characteristic for the α-HQ crystal.

Thus, the IR spectra allow to monitor changes in the β-HQ–Xe crystal during its heating up to the melting at ca. 447 K. In the 298–398 K temperature range the studied sample contains cages filled with the Xe atoms. At 407 K the guest Xe atoms start to leave the host crystal and empty cages are formed. It is followed by the jumping of the γOH band from ca. 670 to 610 cm^{-1}. Internal vibrations of resulting the meta-stable β-HQ* crystal, particularly the IR absorption due to the aromatic ring vibrations in the 1300–1150 cm^{-1} region and at ca. 526 cm^{-1} (ν_{12}, ν_3, ν_{18}, ν_{17}), are characteristic for the β form of HQ. The β-HQ* transforms into its α-HQ modification above 418 K. Thus, we can state that two distinctly different processes: (i) β-HQ–Xe → β-HQ* and (ii) β-HQ* → α-HQ are observed.

The temperature changes observed in the IR spectra of the β-DQ–Xe crystal, produced by its heating up from the room temperature to the Xe escape, are similar in character to those found in the IR spectra of the β-HQ–Xe crystal, however, they are observed in the lower temperature range (Fig. 5, Table S2b). Up to 368 K, only the bands due to the D-bond vibrations exhibit significant shift either to the lower (γOD from 550 to 537 cm^{-1} and δOD from 988 to 981 cm^{-1}) or to the higher (νOD from 2370 to 2386 cm^{-1}) wavenumbers, respectively.

Both the γOD and νOD frequency variations reflect weakening of the ODO bonds with heating of the β-DQ–Xe crystal. The remaining infrared bands, derived from the internal vibrations of the aromatic ring, show the same shapes and positions in the 298–368 K temperature region.

On heating up above 368 K of the β-DQ–Xe crystal, we observe two features: (i) the jumping of the γOD band from 537 cm^{-1} at 368-378 K to ca. 440 cm^{-1} at 373–388 K and (ii) progressive lowering of its value from ca. 440 cm^{-1} at 373–388 K to 427 cm^{-1} at 438 K. These two phenomena are similar to those observed for the β-HQ–Xe crystal and they are attributed to the Xe escape from the β-DQ–Xe crystal at ca. 375 K and the β-DQ* → α-DQ phase transition, respectively. Progressive decrease of the γOD wavenumber after the Xe escape is accompanied by appearance of the bands at: 1256 cm^{-1} (373 K), 1164 cm^{-1} (378 K), 1308 cm^{-1} (378 K) and 1020 cm^{-1} (398 K) being characteristic for the α-DQ modification.

In fact, our TG–DTA experiment confirms this interpretation (Fig. 7). The DTA and TG curves for the β-DQ–Xe crystal are very similar to those obtained for the non-deuterated analogue (Figs. 6 and 7). The most important difference is the bigger temperature difference between the Xe escape and the crystal melting. Thus, in this case, contrary to the β-HQ–Xe crystal, we estimated the sample weight loss due to the Xe escape and the clathrate chemical formula: $C_6H_4D_2O_2 \cdot Xe_{0.22}$ (expected maximum content of the Xe guest is equal to 0.33).

Finally, one should note that the IR spectra of the deuterated sample are more complex than the ones of the non-deuterated sample. In the former case, a small α-DQ contamination is responsible for the additional bands, e.g. its γOD band shifts from 493 to 468 cm^{-1} as the temperature increases from 298 to 388 K and then it disappears above 388 K. It suggests the Xe escape from the α contamination.

4. Summary and conclusions

1. Detailed analysis of the infrared spectra of the β-HQ–Xe and β-DQ–Xe crystals (clathrates) at the room temperature is presented.
2. The temperature evolution of these spectra from 11 to 338–348 K is considered. The most temperature sensitive bands arise from vibrations in which the O–H···O and O–D···O bonds play essential role. On heating up of the crystals, it was found that the γOH and γOD bands shift to lower and the νOH and νOD bands

to higher wavenumbers. Both these effects indicate progressive weakening of the OHO and ODO bonds in hexagonal rings $[\cdots O–H\cdots O–]_6$ and $[\cdots O–D\cdots O–]_6$ (respectively) when the samples are heated from 11 K up to the Xe escape temperatures. Relations between this weakening and the Xe escape need an additional study.

3. The Xe escape from the β-HQ–Xe and β-DQ–Xe crystals was observed by the infrared spectra and was confirmed by TG–DTA experiments. The Xe atom content was estimated from our TG results for the β-DQ–Xe clathrate only—its chemical formula was established as: $C_6H_4D_2O_2{\cdot}Xe_{0.22}$.
4. At ca. 410 K, the Xe guests leave the β-HQ–Xe crystal and empty cages are formed. This is followed by jumping of the γOH band from ca. 670 to 610 cm^{-1}. Internal vibrations of the resulting meta-stable β-HQ* crystal are characteristic for the β-form of hydroquinone.
5. β-HQ* transforms into its α-HQ modification above 418 K and below the melting of the crystal. This process is monitored by formation of the bands characteristic for α-HQ.
6. Analogous processes were observed in the infrared spectra of the β-DQ–Xe crystal. The β-DQ–Xe → β-DQ* transformation proceeds at ca. 375 K and it is followed by the jumping of the γOD band from 537 to ca. 440 cm^{-1}. The β-DQ* → α-DQ transition is also followed by formation of bands characteristic for its α-modification.

Appendix A. Supplementary data

Supplementary data associated with this article can be found, in the online version, at doi:10.1016/j.vibspec.2010.09.005.

References

[1] D.E. Palin, H.M. Powell, J. Chem. Soc. (1947) 208.
[2] St.C. Wallwork, H.M. Powell, J. Chem. Soc. Perkin II (1980) 641.
[3] K. Maartmann-Moe, Acta Cryst. 12 (1966) 979.
[4] T. Birchall, Ch.S. Frampton, G.J. Schrobilgen, J. Valsdóttier, Acta Cryst. C45 (1989) 944.
[5] J.L. Atwood, J.E.D. Davies (Eds.), Inclusion Phenomenon in Inorganic, Organic and Organometallic Hosts, Kluwer Academic Publishers, 1987.
[6] S.C. Cullen, E.G. Gross, Science 113 (1951) 580.
[7] L. Mandelcorn, Chem. Rev. 59 (1959) 827.
[8] J.E.D. Davies, J. Chem. Soc. Dalton Trans. (1972) 1182.
[9] J.E.D. Davies, W.J. Wood, J. Chem. Soc. Dalton Trans. (1975) 674.
[10] R.V. Belosludov, V.R. Belosludov, V.E. Zubkus, J. Chem. Phys. 103 (1995) 2773.
[11] S. Hirokawa, J. Chem. Phys. 80 (1984) 687.
[12] M. Kubinyi, F. Billes, A. Grofcsik, G. Keresztury, J. Mol. Struct. 266 (1992) 339.
[13] M. Kubinyi, G. Keresztury, Mikrochim. Acta 14 (Suppl.) (1997) 525.
[14] J.C. Burgiel, H. Meyer, P.L. Richards, J. Chem. Phys. 43 (1965) 4291.
[15] B.A. Kolesov, G.N. Czechov, Yu.A. Diadin, Zh. Strukt. Chim. 27 (1986) 46.
[16] G. Varsányi, Vibrational Spectra of Benzene Derivatives, Akadémiai Kiadó, Budapest, 1969.
[17] B. Wojtkowiak, M. Chabanel, Spectrochimie Moleculaire, Technique et Dokumentation, Paris, 1977.
[18] M.J. Frisch, G.W. Trucks, H.B. Schlegel, G.E. Scuseria, M.A. Robb, J.R. Cheeseman, J.A. Montgomery, T. Vreven, K.N. Kudin, J.C. Burant, J.M. Millam, S.S. Iyengar, J. Tomasi, V. Barone, B. Mennucci, M. Cossi, G. Scalmani, N. Rega, G.A. Petersson, H. Nakatsuji, M. Hada, M. Ehara, K. Toyota, R. Fukuda, J. Hasegawa, M. Ishida, T. Nakajima, Y. Honda, O. Kitao, H. Nakai, M. Klene, X. Li, J.E. Knox, H.P. Hratchian, J.B. Cross, V. Bakken, C. Adamo, J. Jaramillo, R. Gomperts, R.E. Stratmann, O. Yazyev, A.J. Austin, R. Cammi, C. Pomelli, J.W. Ochterski, P.Y. Ayala, K. Morokuma, G.A. Voth, P. Salvador, J.J. Dannenberg, V.G. Zakrzewski, S. Dapprich, A.D. Daniels, M.C. Strain, O. Farkas, D.K. Malick, A.D. Rabuck, K. Raghavachari, J.B. Foresman, J.V. Ortiz, Q. Cui, A.G. Baboul, S. Clifford, J. Cioslowski, B.B. Stefanov, G. Liu, A. Liashenko, P. Piskorz, I. Komaromi, R.L. Martin, D.J. Fox, T. Keith, M.A. Al-Laham, C.Y. Peng, A. Nanayakkara, M. Challacombe, P.M.W. Gill, V. Johnson, W. Chen, M.W. Wong, C. Gonzalez, J.A. Pople, Gaussian 03, Revision D.01, Gaussian, Inc., Wallingford, CT, 2004.
[19] A. Novak, Struct. Bond. 18 (1974) 177.
[20] J.L. Daschbach, T.-M. Chang, L.R. Corrales, L.X. Dang, P. McGrail, J. Phys. Chem. B110 (2006) 17291.